Bulletin of the Seismological Society of America, Vol. 78, No. 2, pp. 898–907, April 1988

TUNNELING RAYS USING THE CAGNIARD-DE HOOP METHOD

BY G. G. DRIJKONINGEN AND C. H. CHAPMAN

ABSTRACT

Tunneling signals can be studied ideally by application of the Cagniard-de Hoop method. Here, we use this method to derive the response function for the canonical configuration of two acoustic half-spaces, excited by a line source. In order to reveal the characteristics of the tunneling signal, we expand the Cagniard response around the relevant ray parameter and evaluate the associated signal. The result is the nongeometrical arrival due to a tunneling ray. This arrival can be modeled accurately by asymptotic theory when the phase is allowed to be complex (instead of real in the case of geometrical arrivals); a few numerical results illustrate this.

INTRODUCTION

Evanescent waves are often encountered in seismology and also often neglected because of their property of exponential decay. Recently, a few cases have been investigated in which they could not be neglected. One is the so-called S^* arrival to which Hron and others have devoted several publications (Hron and Mikhailenko, 1981; Daley and Hron, 1983; Gutowski *et al.*, 1984; Kim and Behrens, 1986), theoretical as well as experimental. Another example of an evanescent wave, which contributes to the final response, is the direct wave root, an arrival observed by Stephen and Bolmer (1985) in a marine environment.

In the investigations to analyze these arrivals, heavy numerical analysis or unnecessarily complicated methods have often been employed. The Cagniard-de Hoop method is ideal for these arrivals, and it is surprising others have not used it. Here, we shall apply this method to a simple, canonical problem.

We start our discussion by showing a few configurations in which evanescent waves may occur and which can be analyzed using the Cagniard-de Hoop technique. In the remainder of the paper we shall confine ourselves to the canonical problem of two acoustic half-spaces in contact and derive the exact response to line-source excitation. In order to reveal the important features of the total signal, we expand the Cagniard response around the ray parameters of interest and evaluate the signals which are associated with the geometrical and nongeometrical arrivals. The properties of the nongeometrical arrival will be discussed briefly. In the last section, numerical results are used to compare the approximate and exact signals.

EXAMPLES OF TUNNELING RAYS

In the seismological literature, tunneling rays have not been paid as much attention as in the field of optics where research is considerable (e.g., Keller, 1958; Choudhary and Felsen, 1973; Felsen, 1976; Einziger and Raz, 1980). Despite this attention, it is not yet very clear how these phases can be described in generally inhomogeneous media by means of a ray theory. Therefore, we consider only laterally homogeneous media for which ray theory is simpler and other methods are available. Plane-layered media can conveniently be studied by the Cagniard-de Hoop method, especially when one particular arrival is under consideration.

In Figure 1, we have depicted a few examples of tunneling signals in simple-layered media. Figure 1a shows the situation which we consider as our canonical

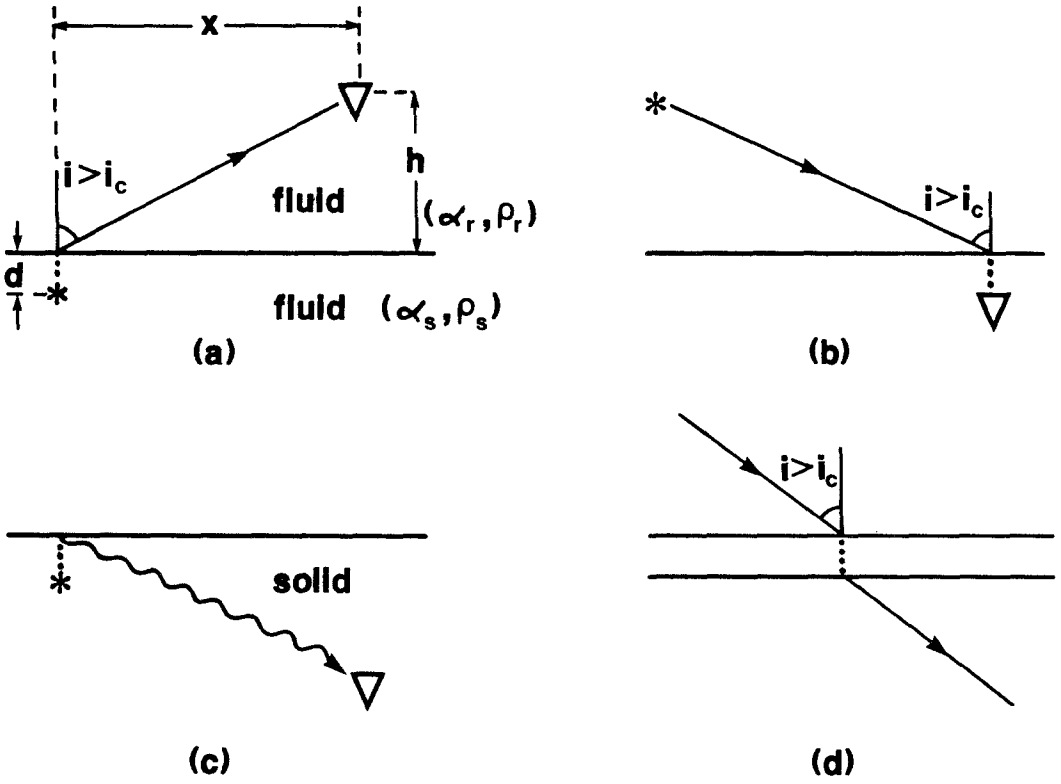

FIG. 1. Four configurations in which evanescent waves can be expected. i_c denotes the critical angle. (a) Canonical configuration, two acoustic half-spaces in contact, d denotes source depth, h receiver depth, and x range; $\alpha_s > \alpha_r$. (b) Reciprocal of configuration (a) where the receiver is in the lower medium near the interface. (c) S^* arrival. (d) A ray impinging postcritically on a high-velocity layer.

problem. It consists of two acoustic half-spaces in contact where a line source is situated near the interface in the medium with the higher wave speed. Tunneling occurs from the source into the other medium.

In Figure 1b, we have drawn the configuration in which the so-called direct wave root may occur. Stephen and Bolmer (1985) gave this name to a nongeometrical arrival encountered in a marine environment, where tunneling can occur through the sea bed which usually has a higher wave speed than the water on top of it. In their case, the receiver was in the sea bed while the source was in the water. This situation is the reciprocal of Figure 1a.

Then we have, as mentioned earlier, the S^* arrival (Figure 1c). This arrival occurs in a solid half-space. The two wave speeds are now the P and S velocities and a P wave tunnels from the source and is reflected as an S wave. This arrival was first noticed in a numerical study by Hron and Mikhailenko (1981), and other theoretical and experimental studies have followed (Daley and Hron, 1983; Gutowski *et al.*, 1984; Kim and Behrens, 1986). Although the properties of the S^* arrival are revealed by these studies, the methods by which they were determined were often unnecessarily complicated.

In Figure 1d, we have illustrated another configuration in which the signal will be influenced by an evanescent part if a ray impinges postcritically on a thin, high-velocity layer. Examples of this situation have been encountered by Hong and Helmberger (1977), Helmberger and Hadley (1981), and Fuchs and Schulz (1976).

Another example of tunneling was investigated by Richards (1973), who discussed evanescent energy tunneling into the core of the earth via waves having a turning point just above the core-mantle boundary. This situation is more complicated and will not be considered here.

As mentioned earlier, all of the situations in Figure 1 can be treated very elegantly by application of the Cagniard-de Hoop technique. We shall focus our attention now on the canonical problem (Figure 1a). Solutions of the other situations are very similar.

The Exact Response for the Canonical Problem

Our canonical problem (Figure 1a) is a line source situated in an configuration which consists of two homogeneous perfectly fluid half-spaces separated by an interface. The origin of the coordinate axes is chosen on the interface with the z axis pointing upwards and the y axis runs parallel to the direction of the line source so the configuration can be treated as two-dimensional. The source is situated on the z axis at a distance d from the interface, embedded in the lower medium with density ρ_s and wave speed α_s. The upper medium is specified by its wave speed α_r and density ρ_r and contains the receiver at range x and depth $z = h$. In this configuration, we have chosen α_s larger than α_r, a specification which we will use later on.

When the source function is taken as a Dirac pulse in time, starting to act at $t = 0$, the incident field for the pressure p^i is governed by the inhomogeneous wave equation

$$\frac{\partial^2 p^i}{\partial x^2} + \frac{\partial^2 p^i}{\partial z^2} - \frac{1}{\alpha_s^2}\frac{\partial^2 p^i}{\partial t^2} = -\delta(x, z + d)\delta(t). \tag{1}$$

We apply a Fourier transformation with respect to the time and x coordinate according to

$$\tilde{p}^i = \int_{-\infty}^{+\infty}\int_{-\infty}^{+\infty} p^i \exp\{i\omega(t - px)\}\, dx\, dt \tag{2}$$

where p can be associated with the horizontal slowness. This will transform the partial differential equation (1) into an ordinary differential equation in the transform domain. The solution of the ordinary differential equation is simple. The solution for the transmitted wave is standard (see, e.g., Aki and Richards, 1980) and only involves applying the radiation condition and the boundary conditions of continuity of pressure and vertical displacement at the interface. We obtain for the transmitted pressure $\tilde{p}^t$

$$\tilde{p}^t = \frac{i}{2\omega q_{\alpha_s}} \exp(i\omega q_{\alpha_s} d) T \exp(i\omega q_{\alpha_r} z) \tag{3}$$

where

$$T = 2\rho_r q_{\alpha_s}/(\rho_r q_{\alpha_s} + \rho_r q_{\alpha_r})$$

$$q_{\alpha_r} = (\alpha_r^{-2} - p^2)^{1/2} \qquad \mathrm{Im}(\omega q_{\alpha_r}) \geqq 0$$

$$q_{\alpha_s} = (\alpha_s^{-2} - p^2)^{1/2} \qquad \mathrm{Im}(\omega q_{\alpha_s}) \geqq 0.$$

We can invert (3) to the space-time domain using de Hoop's modification (de Hoop, 1960) of Cagniard's method (Cagniard, 1939, 1962). All of the details involved can be found in the mentioned works as well as in many recent textbooks (e.g., Aki and Richards, 1980; Ben-Menahem and Singh, 1981; Kennett, 1983). Going from the transform domain to the frequency domain,

$$\hat{p}^t(x, z, \omega) = \frac{i}{4\pi} \int_{-\infty}^{\infty} \frac{T}{q_{\alpha_s}} \exp(i\omega\theta)\, dp \tag{4}$$

where

$$\theta = px + q_{\alpha_s} d + q_{\alpha_r} h.$$

We distort the contour of integration in the complex p domain in such a way that we can identify θ with time t (purely real and positive). The curve $t = \theta$ has been called the Cagniard contour. Knowing that an exponential in the Fourier domain corresponds to a shift in the time domain, we can invert expression (4) to the time domain. Making use of the symmetry of the integrand and evaluating the integral at the discontinuity of the δ-pulse, we arrive at the final (exact) result

$$p^t(x, z, t) = (2\pi)^{-1} \mathrm{Im}\left[\frac{T}{q_{\alpha_s}} \frac{1}{d\theta/dp}\right]_{t=\theta}. \tag{5}$$

The subscript means that for each time value t, the expression $\mathrm{Im}[\cdots]$ must be evaluated at that value of p which solves simultaneously $\mathrm{Re}(\theta) = t$ and $\mathrm{Im}(\theta) = 0$. Although equation (5) gives the exact answer to our problem, it does not show its features very clearly. Therefore, we will have a closer look at the Cagniard contour.

If the source is near the interface (in the medium with the higher wave speed) and the receiver is at a far range, a typical contour is illustrated in Figure 2. It shows two main features. One is the part of the curve near A which departs from the intersection point with the real axis but remains near to the axis. At the point

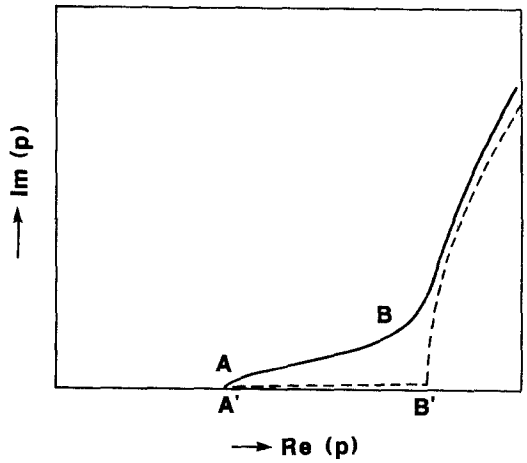

FIG. 2. A typical Cagniard contour in the complex p plane. Note the important features: the intersection with the real p axis (geometrical arrival) and the bend (nongeometrical arrival). The dashed line is the contour if the source was on the interface.

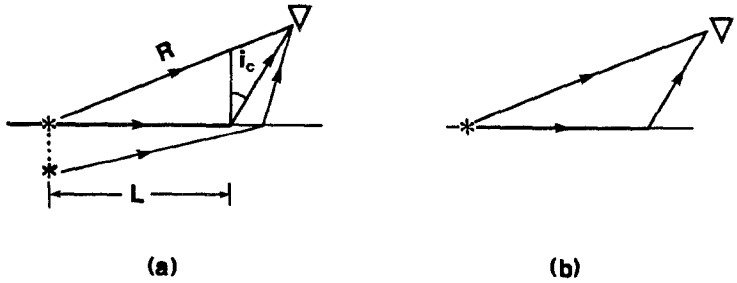

FIG. 3. The geometrical interpretations of L and R. (a) The two rays joining source and receiver. R is the distance traveled by the direct ray and L the distance traveled by the head wave along the interface if the source was on the interface (b).

of intersection, $d\theta/dp = 0$, and this corresponds to the geometrical arrival (Figure 3a) which satisfies Snell's law. Ultimately, if the source were placed on the interface, the part of the curve near the real axis would lie on that axis (curve $A'B'$). It would contribute to the response due to the branch-point of q_{α_s}, well-known to be the cause of head waves (Figure 3b) (Jeffreys, 1926; Aki and Richards, 1980). The second feature is the part of the curve which bends away from the real axis more rapidly near B. If the source were placed on the interface, the contour would now depart from the real axis at B'. This would correspond to the direct geometrical arrival (Figure 3b).

We shall now investigate the signals associated with the two regions by expanding around the ray parameters of interest, i.e., $p_1 = 1/\alpha_s$ and $p_2 = \sin i/\alpha_r$.

THE EXPANSIONS

In this section, we will assume that the source depth is small compared to the receiver depth, i.e., $d \ll h$. We start with the expansion around the intersection point: $p = p_1 + \delta$. Keeping only first-order terms in the expression for the contour $t = \theta$, we can solve for the small parameter δ

$$\delta = \frac{t - \tau_h}{L} \tag{6}$$

where L has the geometrical interpretation as given in Figure 3a, and τ_h is the travel time of the head wave if the source were on the interface. Apart from the term q_{α_s} which is present in the transmission factor as well as in $d\theta/dp$, all of the terms in expression (5) are evaluated at p_1. Our signal will be

$$p^t_{geom} \simeq \frac{1}{\pi L}\frac{\rho_r}{\rho_s q_r}\left(\frac{p_1}{2L}\right)^{1/2} H(t-\tau_h)\left\{\frac{2\rho_r}{\rho_s q_r}(t-\tau_h)^{1/2} + d(t-\tau_h)^{-1/2}\right\} \tag{7}$$

where q_r is q_{α_r} evaluated at p_1 and $H(t)$ denotes the Heaviside step function. It can readily be seen that the signal consists of a combined contribution of a head wave-type arrival and a geometrical arrival. The incident pulse is $p^i \simeq (1/2\pi)(\alpha_s/2r)^{-1/2}$ $H(t - r/\alpha_s)(t - r/\alpha_s)^{-1/2}$, where r is the ray length. The head wave has a range dependence of $L^{-3/2}$ and a pulse shape which is the integral of the incident pulse. The transmitted geometrical arrival is just a scaled version of the incident pulse. Ultimately, when the source depth d goes to zero, we will only have the contribution

from the head-wave term, while the geometrical term will dominate when the source depth is large.

The other region of interest in the complex p plane is around the point on the real axis near the bend of the Cagniard contour, $p_2 = \sin i/\alpha_r$. This point has been recognized as significant before (e.g., Hong and Helmberger, 1977), but further analysis has not been performed. Again we will solve for the Cagniard contour, taking $p = p_2 + \epsilon$ for the ray parameter. Expanding the vertical wave slowness, q_{α_r}, and keeping second-order terms (as the first-order terms vanish, see also Figure 3b), we solve for the small parameter ϵ

$$\epsilon = i\alpha_r q_r \left(\frac{2q_r}{h}\right)^{1/2} (t - R/\alpha_r - iq_s d)^{1/2} \tag{8}$$

where q_r and q_s are the vertical wave slownesses evaluated at p_2 and R has the geometrical interpretation depicted in Figure 3b. In order to evaluate the signal, we must separate the root of the complex term in equation (8) into a real and imaginary part

$$\begin{aligned}(t-R/\alpha_r-iq_sd)^{1/2} &= u+iv \\ &= [\{(t-R/\alpha_r)^2+q_s{}^2d^2\}^{1/2}+(t-R/\alpha_r)]^{1/2}/\sqrt{2} \\ &\quad -i[\{(t-R/\alpha_r)^2+q_s{}^2d^2\}^{1/2}-(t-R/\alpha_r)]^{1/2}/\sqrt{2}. \end{aligned} \tag{9}$$

The important term in the Cagniard-de Hoop result (5) is $d\theta/dp$ while the other terms are evaluated at $p = p_2$ and are treated as constants. The final result will be

$$\begin{aligned} p^t_{ev} &\simeq \frac{1}{\pi}\frac{\rho_r}{\rho_r{}^2q_s{}^2+\rho_s{}^2q_r{}^2}\left(\frac{p_2}{2x}\right)^{1/2}\frac{\alpha_r q_r(\rho_s q_r u-\rho_r q_s v)}{\{(t-R/\alpha_r)^2+q_s{}^2d^2\}^{1/2}} \\ &= \frac{1}{\pi^2}\frac{\rho_r(\rho_s q_r+\rho_r q_s)}{\rho_r{}^2q_s{}^2+\rho_s{}^2q_r{}^2}\left(\frac{p_2}{2x}\right)^{1/2}\alpha_r q_r q_s d \qquad (10a) \\ &\quad \times H(t-R/\alpha_r)(t-R/\alpha_r)^{1/2} * (t^2+q_s{}^2d^2)^{-1} \qquad (10b) \end{aligned}$$

where the asterisk denotes convolution. That (10a) and (10b) are equal is most easily established in the Fourier domain. The transform of (10a) can be found in tables of integral transforms [Erdélyi, 1954, equations (1.3.22) and (2.3.20)]

$$\begin{aligned} F\left\{\frac{u}{[(t-R/\alpha_r)^2+q_s{}^2d^2]^{1/2}}\right\} &= \left(\frac{\pi}{\omega}\right)^{1/2}\exp(i\pi/4)\exp(i\omega(R/\alpha_r+iq_sd)) \\ F\left\{\frac{-v}{[(t-R/\alpha_r)^2+q_s{}^2d^2]^{1/2}}\right\} &= \left(\frac{\pi}{\omega}\right)^{1/2}\exp(-i\pi/4)\exp(i\omega(R/\alpha_r+iq_sd)) \end{aligned} \tag{11}$$

where $\omega > 0$, and we have made use of the fact that for the order $\frac{1}{2}$, the modified Bessel function reduces to the simple exact form [Watson, 1958, p. 80 equation (13)]

$$K_{1/2}(\omega q_s d) = \left(\frac{\pi}{2\omega q_s d}\right)^{1/2} \exp(-\omega q_s d). \tag{12}$$

We have now completely resolved the important features: the slightly complicated form in expression (10a) is just the incident field convolved with a function of the type $(t^2 + q_s^2 d^2)^{-1}$ which corresponds to a multiplication in the frequency domain by $\exp(-|\omega| q_s d)$.

Thus, by expanding about the appropriate point of the Cagniard contour, we have approximated the exact response and obtained a simple expression for a tunneling signal. In the frequency domain, it is described by a complex phase with the expected evanescent decay.

The properties of tunneling signals follow easily. These have been mentioned before (Daley and Hron, 1983; Stephen and Bolmer, 1985) but some inconsistencies have slipped into them, so for completeness we state them again

1. The approximate signal is acausal.
2. The arrival only exists in a limited region. This region is always associated with a postcritical phenomenon; in our canonical problem, it means that q_{α_s} becomes complex for $p > 1/\alpha_s$.
3. The signal will consist of a scaled incident field with time delay R convolved with a function of the type $(t^2 + I^2)^{-1}$ in accordance with a complex phase $R + iI$ in the Fourier domain. [Stephen and Bolmer (1985) say on p. 61, "The 'direct wave root' is a wave of second order and has a wave form proportional to the integral of the incident wave form." They do not justify their statement, and we are uncertain of the reasoning.]

Numerical Results

The theoretical results presented in the last section are self-explanatory. In order to investigate the validity of the approximations, we compare exact and approximate results numerically. The exact and the approximate results contain an inverse square root singularity at the arrival time of the geometrical arrival. By taking a finite sampling width, we have smoothed our results so the singularity may not show.

In Figure 4, we have chosen a low impedance contrast while in Figure 5 this contrast is higher. The values of the parameters are given in the figure legends. When the source depths are small (Figures 4a and 5a), the smoothed first arrival is dominated by the head-wave term, and the nongeometrical arrival behaves almost like $H(t)t^{-1/2}$. An increase in source depth (Figures 4b and 5b) will increase the influence of the geometrical term in the first arrival. A large source depth (Figures 4c and 5c) will give us the singularity for the geometrical arrival, even after smoothing. For the nongeometrical arrival, we now have a pulse smoothed by its convolution with the function $(t^2 + q_s^2 d^2)^{-1}$.

For the geometrical arrival, we notice that the approximation is almost perfect for all of the source depths. The approximation for the nongeometrical arrival is less good, but it should be emphasized that we are dealing with two different rays. Each of the approximations has its own region of applicability, and outside these

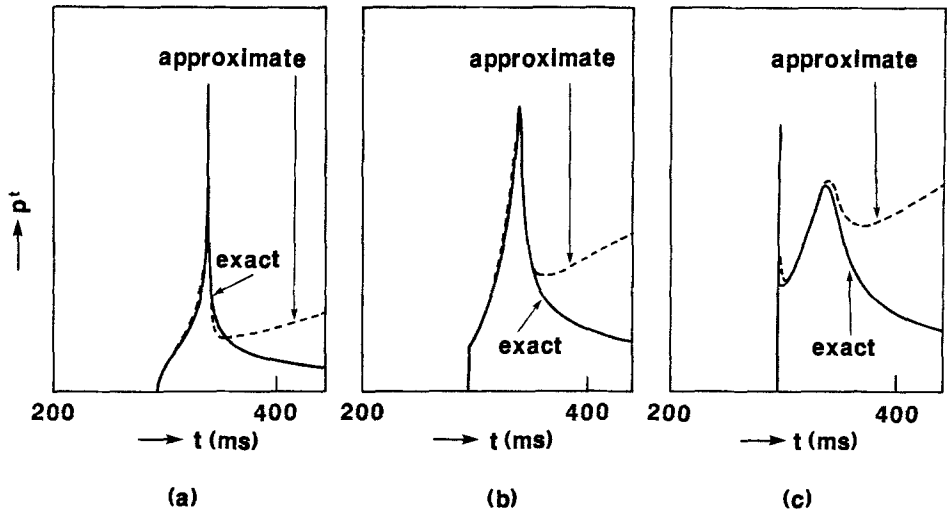

FIG. 4. Exact and approximate (smoothed) signals for low impedance contrast: $\alpha_s/\alpha_r = 1.33$, $\rho_s/\rho_r = 1.2$, (receiver depth) $h = 100$ m, and (range) $x = 500$ m. The source depth d differs for each figure: (a) $d = 1$ m; (b) $d = 7.5$ m; and (c) $d = 30$ m. A DC value of the amplitude of the approximate evanescent wave at the time of the first arrival has been subtracted from the whole trace.

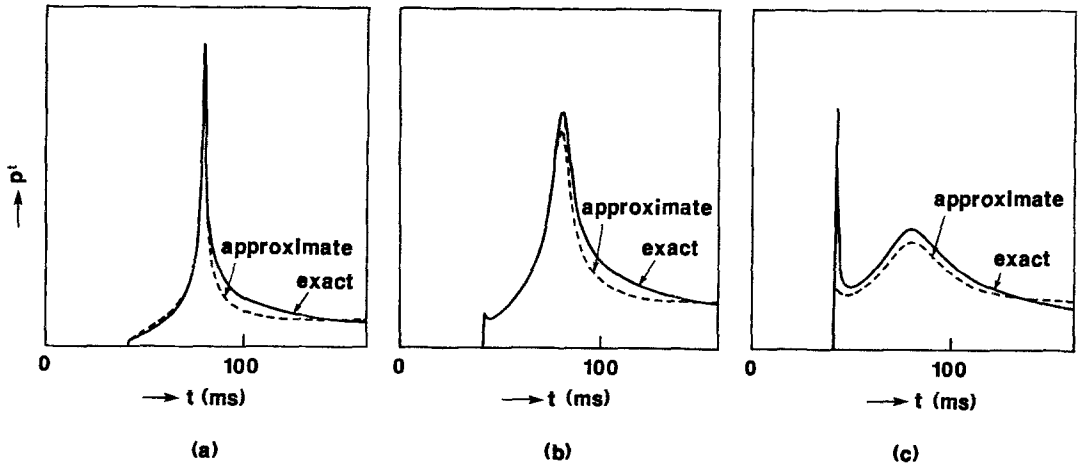

FIG. 5. Exact and approximate (smoothed) signals for high impedance contrast: $\alpha_s/\alpha_r = 2$ and $\rho_s/\rho_r = 2$. Apart from a range x of 250 m, all of the other parameters have the same value as in Figure 4. Again, note that a DC value of the amplitude of the evanescent wave at the time of the first arrival has been subtracted from the whole trace.

regions a contribution is still present, so influencing the signal due to the other ray. For convenience, we have taken the contribution of the nongeometrical arrival equal to zero before the time of the first arrival, and the value of the nongeometrical arrival at the time of the first arrival is subtracted from the rest of the trace. Thus, the actual fit for the evanescent wave is not shown in these figures, as the contribution of the geometrical arrival extends beyond its region of applicability into the region where the evanescent wave is important. This is why we have included Figure 6, in which we have taken the contribution of the tunneling ray only, and we have made no corrections for causality. It can be seen that the fit is now better.

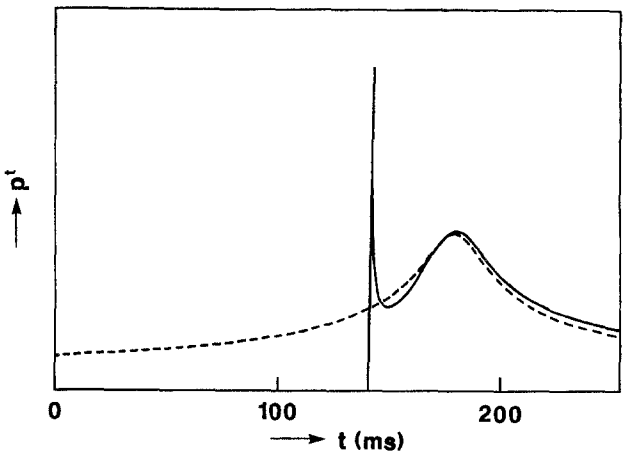

FIG. 6. The comparison between the exact signal and the acausal nongeometrical arrival without corrections. The approximation for the geometrical arrival has not been included. Parameter values are the same as in Figure 5c.

CONCLUSIONS

Tunneling rays in plane-layered homogeneous media can be studied ideally by application of the Cagniard-de Hoop method from which the very nature of the ray can be revealed by expanding the Cagniard contour around the ray parameters of interest. In the canonical problem of two acoustic half-spaces, we have two ray parameters which give rise to arrivals. The first arrival is the geometrical arrival which tends to a head wave when the source approaches the interface (7), while the other arrival is nongeometrical with a signal which is a smoothed version of the incident field but tends to the (scaled) incident field when the source approaches the interface (10).

We have seen that, for homogeneous media with plane interfaces, asymptotic theory is a good approximation for tunneling rays when the phase is allowed to be complex. This characteristic is used as the starting point for complex ray tracing in generally inhomogeneous media (Choudhary and Felsen, 1973; Felsen, 1976). More research on the behavior of tunneling rays in more general media is obviously needed.

REFERENCES

Aki, K. and P. G. Richards (1980). *Quantitative Seismology*, vol. I, W. H. Freeman and Co., San Francisco, California, 768 pp.

Ben-Menahem, A. and S. J. Singh (1981). *Seismic Waves and Sources*, Springer-Verlag, New York.

Cagniard, L. (1939). *Réflection and Réfraction des Ondes Séismiques Progressives*, Gauthiers-Villars, Paris, France.

Cagniard, L. (1962). *Reflection and Refraction of Progressive Seismic Waves*, translated from French by E. A. Flinn and C. H. Dix, McGraw-Hill, New York.

Choudhary, S. and L. B. Felsen (1973). Asymptotic theory for inhomogeneous waves, *IEEE Trans. Ant. Prop.* **AP-21**, 827–842.

Daley, P. F. and F. Hron (1983). High-frequency approximation to the nongeometrical S^* arrival, *Bull. Seism. Soc. Am.* **73**, 109–123.

de Hoop, A. T. (1960). A modification of Cagniard's method for solving seismic pulse problems, *Appl. Sci. Res.* **B8**, 349–356.

Einziger, P. and S. Raz (1980). On the asymptotic theory of inhomogeneous wave tracking, *Radio Sci.* **15**, 763–771.

Erdélyi, A. (1954). *Tables of Integral Transforms*, vol. I, McGraw-Hill, New York.

Felsen, L. B. (1976). Evanescent waves, *J. Opt. Soc. Am.* **66,** 751–760.

Fuchs, K. and K. Schulz (1976). Tunneling of low-frequency waves through the subcrustal lithosphere, *J. Geophys.* **42,** 175–190.

Gutowski, P. R., F. Hron, D. E. Wagner, and S. Treitel (1984). *S**, *Bull. Seism. Soc. Am.* **74,** 61–78.

Helmberger, D. V. and D. M. Hadley (1981). Seismic source functions and attenuation from local and teleseismic observations of the NTS events Jorum and Handley, *Bull. Seism. Soc. Am.* **71,** 51–67.

Hong, T.-L. and D. V. Helmberger (1977). Generalized ray theory for dipping structure, *Bull. Seism. Soc. Am.* **67,** 995–1008.

Hron, F. and B. G. Mikhailenko (1981). Numerical modeling of nongeometrical effects by the Alekseev-Mikhailenko method, *Bull. Seism. Soc. Am.* **71,** 1011–1029.

Jeffreys, H. (1926). On compressional waves in two superposed layers, *Proc. Camb. Phil. Soc.* **23,** 472–481.

Keller, J. B. (1958). Calculus of variations and its applications, in *Proceedings of Symposia in Applied Mathematics*, vol. VIII, L. M. Graves, Editor, McGraw-Hill, New York, 27–52.

Kennett, B. L. N. (1983). *Seismic Wave Propagation in Stratified Media*, Cambridge University Press, Cambridge, England.

Kim, J. Y. and J. Behrens (1986). Experimental evidence of the *S** wave, *Geophys. Prosp.* **34,** 100–108.

Richards, P. G. (1973). Calculations of body waves, for caustics and tunneling in core phases, *Geophys. J. R. Astr. Soc.* **35,** 243–264.

Stephen, R. A. and S. T. Bolmer (1985). The direct wave root in marine seismology, *Bull. Seism. Soc. Am.* **75,** 57–67.

Watson, G. N. (1958). *A Treatise on the Theory of Bessel Functions*, 2nd ed., Cambridge University Press, Cambridge, England.

BULLARD LABORATORIES
DEPARTMENT OF EARTH SCIENCES
UNIVERSITY OF CAMBRIDGE
CAMBRIDGE CB3 0EZ, UNITED KINGDOM
CONTRIBUTION NO. 1027

Manuscript received 4 July 1987